We are IntechOpen, the world's leading publisher of Open Access books Built by scientists, for scientists

4,800
Open access books available

122,000
International authors and editors

135M
Downloads

Our authors are among the

154
Countries delivered to

TOP 1%
most cited scientists

12.2%
Contributors from top 500 universities

CLARIVATE ANALYTICS BOOK CITATION INDEX INDEXED

WEB OF SCIENCE™

Selection of our books indexed in the Book Citation Index in Web of Science™ Core Collection (BKCI)

Interested in publishing with us?
Contact book.department@intechopen.com

Numbers displayed above are based on latest data collected.
For more information visit www.intechopen.com

5

Anisotropic Kepler Problem and Critical Level Statistics

Kazuhiro Kubo and Tokuzo Shimada
Department of Physics, School of Science and Technology, Meiji University
Japan

1. Introduction

The subject of this chapter is quantum chaos (QC), in particular, the QC that occurs in the Anisotropic Kepler Problem (AKP). In QC, one studies a quantum system whose classical counter part is chaotic, and one investigates how the chaotic property in the classical theory shows up its imprints in the quantum theory. To elucidate this quantum-classical correspondence is the first mission of the quantum chaos study.

With the advent of nanophysics techniques, QC has become very important concern also at the experimental side; for pioneering works, we refer to conductance fluctuations in quantum dot (Marcus et. al., 1992), magnetoresistance on a superlattice of antidots (Weiss et al., 1991), a cold-atom realization of the kicked top (Chaudhury et al., 2009).

Also for an interesting experimental observation of quantum scars of classical orbits (Heller, 1984; 1989), we refer to (Stein & Stöckmann, 1992).

Furthermore, quantum chaos study has been developed under far-reaching mutual influences with related areas. In order to explain where our study in AKP stands, let us briefly review a few aspects of quantum chaos study.

Let us first consider the random matrix theory (RMT) (Mehta, 2004). It is proposed by (Wigner, 1951) to predict the universal spectral property of complex nucleus, and the mathematical basement is set by (Dyson, 1962), (Dyson & Mehta, 1963) and (Mehta & Dyson, 1963). In RMT, the hamiltonian of the physical system is described by a random matrix in the three basic ensembles. This implies that the intrinsic quantum property of the physical system is determined by the time reversal symmetry and internal symmetry only, and does not depend on the details of the system hamiltonian. If the time-reversal by the operator T is broken in a system, the relevant ensemble is gaussian random ensemble of hermite matrices for the hamiltonian, admitting the invariance of the hamiltonian under the unitary transformation (GUE), with Dyson parameter $\beta = 2$. If the T invariance holds with $T^2 = 1$, it is gaussian orthogonal ensemble (GOE) of real symmetric matrices with $\beta = 1$, while with $T^2 = -1$, it is gaussian symplectic ensemble (GSE) of quarternion selfdual matrices with $\beta = 4$. It is conjectured by (Bohigas et al., 1984) that, irrespective to the details of the system hamiltonian, the stochastic spectral property of energy levels of an physical system (including AKP) is uniquely described by the relevant RMT ensemble chosen by the above symmetry property

only, provided that the quantum system is in the ergodic regime (BGS conjecture). [1] This conjecture[2] most remarkably asserts universality classes in the whole lots of quantum chaos systems, and has been successful in great many physical systems [3]. Now, let us mention a famous, though ever charming episode; a mathematician Montgomery was introduced to Dyson at a tea time and explained his result on the spacing distribution of the non-trivial zeros of Riemann zeta function. Then, Dyson immediately told that it is just what he knows, the $P(s)$ of GUE! Of course, one should also mention that the Gutzwiller trace formula that enumerates the semi-classically quantum Green function of a classically chaotic system from unstable periodic orbits has so close intriguing correspondence with the trace formula of the Riemann zeta function (Bohigas, 2005). A deep correspondence between the Riemann zeta function and the random matrix theory is shown by the agreement between the Conrey-Ghosh conjecture on the 2k-th continuous moment of $\zeta(1/2+it)$ and Keating-Snaith random matrix calculation. One of the most flourishing areas in physics is Anderson localization (Evers & Mirlin, 2008) which is only understandable as a quantum phenomena from the interfering amplitudes at the metal and insulator transition point. The critical statistics is a target of critical random matrix theories. So much for general review and let us turn to AKP.

In this chapter, we calculate the energy level statistics of AKP, and find that it is described well (over a finite range of mass anisotropy) by the critical random matrix model devised by (García-García & Verbaarschot, 2003) that is also related to the critical level statistics in the Anderson localization. We also investigate the systematic change of the AKP wave functions with the mass anisotropy. In the Anderson localization, the theory predicts that at the mobility edge, the wave function is multi-fractal, and the level statistics indicator $\Sigma^2(L)$ should show a linear rise for large L that is also observed by our data. In this way, our study may give a support to the recent notion *Anderson localization in quantum chaos* proposed by (García-García, 2007; García-García & Wang, 2008).

The AKP is a system of an electron bound to a proton, just like a hydrogen atom, but the electron has an anisotropic mass. This system is experimentally realized by an electron in a doped semiconductor. Gutzwiller, who made the periodic orbit theory by his semi-classical trace formula, chose often AKP for a nice testing ground of QC (Gutzwiller, 1971; 1977; 1980; 1981; 1982; 1990). In fact, when mass anisotropy is not present, the system is the hydrogen atom (the Kepler problem) that is one of the most well-studied integrable quantum system. By varying the mass anisotropy parameter, the classical system changes the strength of randomness. It is known that the AKP is not KAM system (García-García & Verbaarschot, 2003; Wintgen & Marxer, 1988) that means that the classical phase space, when the mass anisotropy is present, is *not* a mixture of integrable regions (tori) and ergodic regions. Instead, with the increase of the anisotropy, the system changes its classical phase space structure due to the gradual collapse of tori, via the structure filled by cantori (Zaslavsky et al., 1991) (stochastic web of chaos), finally to that filled by isolated unstable periodic orbits. Thus, AKP is really a nice testing ground that gives us the opportunity to investigate how systematically,

[1] The ergodic regime is defined by as the region with $E_c >> \Delta$ where E_c is the Thouless energy $E_c = \hbar D/L^2$ (D is the diffusion constant and L is the system size) and Δ is the mean level spacing.

[2] Recently, a generating function described by a set of periodic orbits is shown, in the semi-classical limit, equivalent to the Feynman diagrams for the kernel in the random matrix theory (Heusler et al., 2007). This clarifies the way the random matrix theory describes the quantum chaos system in the semi-classical limit.

[3] More detailed universality classification is given by (Zirnbauer, 1996).

along with increasing anisotropy, the quantum feature changes reflecting the change in the classical phase space structure. Any periodic orbits in AKP in the chaotic regime can be uniquely coded by its own Bernoulli sequences and furthermore Gutzwiller found an amazing approximate formula that gives the action of a periodic orbit from its Bernoulli sequences.
In this chapter we aim to view various faces of QC from AKP taking the above mentioned advantages of AKP.
In section 2, we first calculate the energy levels of AKP at various anisotropy following the method developed and first applied to AKP by (Wintgen et al., 1987). In this method, there is a particular parameter ϵ (see (6)) and how to choose it at given anisotropy is crucial to guarantee the accuracy of the levels. We use the Sturmian basis just as in (Wintgen et al., 1987) and we present a couple of simple rules to choose the parameter at a given anisotropy. Also, we set up another formulation based on the harmonic oscillator basis. This provides us with a useful check of our results and, in addition, serves as an efficient method for calculating Husimi function that is an important measure to explore the quantum and classical correspondence.
In section 3, we investigate the level statistics in AKP. There is a concrete result by (Wintgen & Marxer, 1988) for the anisotropy parameter $\gamma = 0.8$ (only), but, in order to investigate the quantum statistics change according to the the variation of γ, we definitely need reliable eigenvalue set at various anisotropy too. This is why we have performed the eigenvalue analysis from scratch as described in section 2. We now show for the first time how the number variance and the spectral rigidity change their feature with the variation of mass anisotropy in AKP. The AKP is a system that preserves the time reversal invariance with $T^2 = 1$ and hence its level statistics is expected to be described by GOE in the ergodic region ($\gamma \ll 1$), while in the vicinity of Kepler limit ($\gamma = 1$), it should be Poissonian. We are interested in the physics in the intermediate range. (García-García & Verbaarschot, 2003) showed that the level statistics of AKP at one particular anisotropy is successfully explained by a critical random matrix theory that has one parameter h (temperature in an equivalent model), using the eigenvalue set at $\gamma = 0.8$ given by Wintgen only available at that time, provided that h is suitably chosen. We show that the AKP level statistics can be well described by their critical random matrix theory in a finite range of γ in the intermediate region and show that there is a smooth relation between the parameter h and the anisotropy γ ($h \propto e^{7.2\gamma}$).
In section 4, we now turn our attention to various interesting features of wave functions of AKP. We discuss firstly the nodal line systematics. Then we investigate the probability densities and find salient scars of periodic orbits. This observation is strengthened by the subsequent study of Husimi functions of AKP calculated by the method developed in subsection 4.3.
In section 5, we conclude after a briefly discussion on the future outlook of our work, especially, on the possibility to consider quantum chaos in AKP in the context of Anderson transition

2. Non-perturbative matrix method for the evaluation of quantum energy levels

2.1 WMB method

First we recapitulate the WMB method in the context of AKP (Wintgen et al., 1987; Wintgen & Marxer, 1988) with the electron mass tensor $\mathrm{diag}(m_1, m_1, m_2)$ when diagonalized and mass

anisotropy parameter is $\gamma = m_1/m_2 < 1$. [4]
Introducing appropriate dimensionless coordinates (x, y, z) and momenta (p_x, p_y, p_z), the AKP hamiltonian is

$$\hat{H} = -\left(\frac{\partial^2}{\partial x^2} + \frac{\partial^2}{\partial y^2} + \gamma\frac{\partial^2}{\partial z^2}\right) - \frac{2}{r} \tag{1}$$

$$= -\Delta^{(3)} - \frac{2}{r} + (1-\gamma)\frac{\partial^2}{\partial z^2} \tag{2}$$

in the units $\hbar^2 K/m_1 e^2$, $m_1 e^4/2\hbar^2 K^2$, $2\hbar^3 K^2/m_1 e^4$ for length, energy, time, respectively(K is the dielectric constant). One uses Sturmian basis $\{|n\ell m\rangle\}$

$$\langle \vec{r}|n\ell m\rangle = \frac{1}{r}\sqrt{\frac{n!}{(2\ell+n+1)!}}e^{-\frac{\lambda r}{2}}(\lambda r)^{\ell+1}L_n^{2\ell+1}(\lambda r)Y_{\ell m}(\theta,\varphi). \tag{3}$$

Here n, ℓ, m are radial, azimuthal, magnetic quantum numbers respectively and they are related to the principle quantum number n_p by $n_p = n + \ell + 1$. The parameter λ is introduced for the scaling of r. (In the left hand side the dependence on λ is suppressed for simplicity). Note for the eigen function with n_p in the Kepler problem ($\gamma = 1$), $\lambda = 2/n_p$. In the Sturmian basis the Schrödinger equation of the AKP becomes a matrix equation:

$$\left[-\lambda\overleftrightarrow{\Delta^{(3)}} + (1-\gamma)\lambda\overleftrightarrow{\partial^2/\partial z^2} - 2(\overleftrightarrow{1/r})\right]\mathbf{\Psi} = (E/\lambda)\overleftrightarrow{\mathrm{Id}}\,\mathbf{\Psi} \tag{4}$$

where the eigenvector $\mathbf{\Psi}$ is Col.$(\langle n\ell m|\mathbf{\Psi}\rangle)$, and the matrix elements are respectively

$$\langle n'\ell'm'|\overleftrightarrow{\mathrm{Id}}\,|n\ell m\rangle = \delta_{\ell'\ell}\delta_{m'm}[2(n+\ell+1)\delta_{n'n} - \sqrt{(n+1)(2\ell+n+2)}\delta_{n'n+1}],$$
$$\langle n'\ell'm'|\overleftrightarrow{\Delta^{(3)}}|n\ell m\rangle = (-1)^{n+n'+1}\frac{1}{4}\langle n'\ell'm'|\overleftrightarrow{\mathrm{Id}}\,|n\ell m\rangle,$$
$$\langle n'\ell'm'|\overleftrightarrow{\frac{1}{r}}\,|n\ell m\rangle = \delta_{n'n}\delta_{\ell'\ell}\delta_{m'm}.$$

(The ∂^2 term is somewhat complicated and we refer the reader to (Wintgen et al., 1987)). Noting that the Coulombic interaction term is diagonal, while $\overleftrightarrow{\mathrm{Id}}$ is not, one exchanges them between right and left to obtain the standard eigenvalue problem. Dividing the whole equation by λ one obtains

$$\overleftrightarrow{M}\mathbf{\Psi} \equiv \left[-\overleftrightarrow{\Delta^{(3)}} + (1-\gamma)\overleftrightarrow{\partial^2/\partial z^2} - \epsilon\overleftrightarrow{\mathrm{Id}}\right]\mathbf{\Psi} = (2/\lambda)\mathbf{\Psi}. \tag{5}$$

Note that E/λ in the right-hand side of (4) is now (after divided by λ) changed into a parameter ϵ in the left-hand side of (5), namely

$$E/\lambda^2 \Rightarrow \epsilon. \tag{6}$$

This ϵ should be fixed at some constant value in the diagonalization of (5). This fixing is an extremely clever way in WMB. We will explain this point shortly below.

[4] For ordinary Kepler problem γ is unity; for silicon $\gamma = 0.2079$ and for germanium $\gamma = 0.05134$.

The 'hamiltonian' matrix $\overleftrightarrow{M}$ is symmetric and block diagonal; nonvanishing elements are those with $\ell' = \ell + 2$ or ℓ, and due to the rotational symmetry about z-axis $m' = m$. Therefore one can organize $\overleftrightarrow{M}$ as a banded and sparse matrix. By solving (5) for the eigenvalues $\Lambda_i \equiv 2/\lambda_i$ the energy levels are in turn determined by $E_i = \epsilon\lambda_i^2$. This is the WMB method. In this scheme (5), the eigen function $\langle\vec{r}|\mathbf{\Psi_i}\rangle$ of the i-th level E_i is calculated from the eigen vector $\mathbf{\Psi_i}$ using the Sturmian basis with parameter $\lambda_i = (E_i/\epsilon)^{1/2}$. To be explicit one calculates

$$\langle\vec{r}|\mathbf{\Psi_i}\rangle = \sum_{n,\ell,m} \langle\vec{r}|n\ell m;\lambda_i\rangle\langle n\ell m;\lambda_i|\mathbf{\Psi_i}\rangle. \tag{7}$$

This is in a sharp contrast to (4) where eigenstates of all energy levels must be calculated with a uniquely chosen λ. With the flexibility of *optimizing* λ_i for each $\mathbf{\Psi_i}$, WMB method (5) is by far superior to (4). For instance, if $\gamma \approx 1$, $\epsilon \approx -1/4$ is a good choice since at $\epsilon = -1/4$ the Sturmian basis is already the proper basis for the first order perturbation theory for AKP in $1-\gamma$. [5] In fact we can accommodate various γ by adjusting ϵ properly. Supposing that we choose another value for the parameter ϵ of the matrix $\overleftrightarrow{M}$, the eigenvalues Λ_is will be accordingly changed, but the physical energies E_i should be kept unchanged. However in practice we cannot help using a truncated basis. We discuss how to accommodate this subtle problem by adjusting ϵ shortly below.

Hereafter we focus our attention to the $m = 0$ sector that is related to the $2-$dimensional classical AKP. Also for definiteness we consider the case of even ℓ case. With these constraints the matrix $\overleftrightarrow{M}$ to diagonalize is $N \times N$ with $N = (N_p+1)^2/4$ where N_p is the maximal principal quantum number of the Sturmian basis $\{|n\ell m\rangle\}$, i.e. $n_p = n + \ell + 1 \leq N_p$, $(\ell \leq n_p - 1)$.

We present in Fig. 1 the energy levels of $m = 0$ sector obtained by diagonalizing the 'hamiltonian' $\overleftrightarrow{M}$ in (5) with $N = 7921$ ($N_p = 177$). The levels are plotted as functions of the scaling parameter ϵ (see (5)) for typical values of anisotropy parameter γ, after proper stretch (Bohigas, 2005) using Thomas-Fermi approximation $N(E)$ for the stair case function of AKP (Wintgen & Marxer, 1988)

$$N(E) \equiv \int_{-\infty}^{E} dE'\rho(E') \approx -\frac{1}{4\sqrt{\gamma}E} \tag{8}$$

where $\rho(E) \equiv \sum_i \delta(E - E_i)$ is the level density. Given $N(E)$, the stretched energy levels f_i are given by inversion (unfolding map (Bohigas & Giannoni, 1984));

$$f_i = N(E_i), \;\; i = 1, \cdots, N \tag{9}$$

and the average energy spacing $\langle f_{i+1} - f_i\rangle = 1$. The levels must be independent from the scaling parameter ϵ (level curves must be *horizontal*) in so far as the matrix formalism works properly. (Recall that the WMB method is not a perturbation theory; it should yield exact results if the matrix size N is infinity at any choice of ϵ.) However, at a glance, one finds that the curves are under all over systematic distortion induced by truncating the matrix size. In order to accommodate this, one should select the part of calculated energy levels that satisfy

[5] At $\epsilon = -1/4$ and $\gamma = 1$, $\lambda_i = (E_i/\epsilon)^{1/2} = 2/n_p$ so that $L_n^{2\ell+1}(\lambda_i r) = L_n^{2\ell+1}((2/n_p)r)$ is the main radial part of the eigenfunction of the Kepler problem.

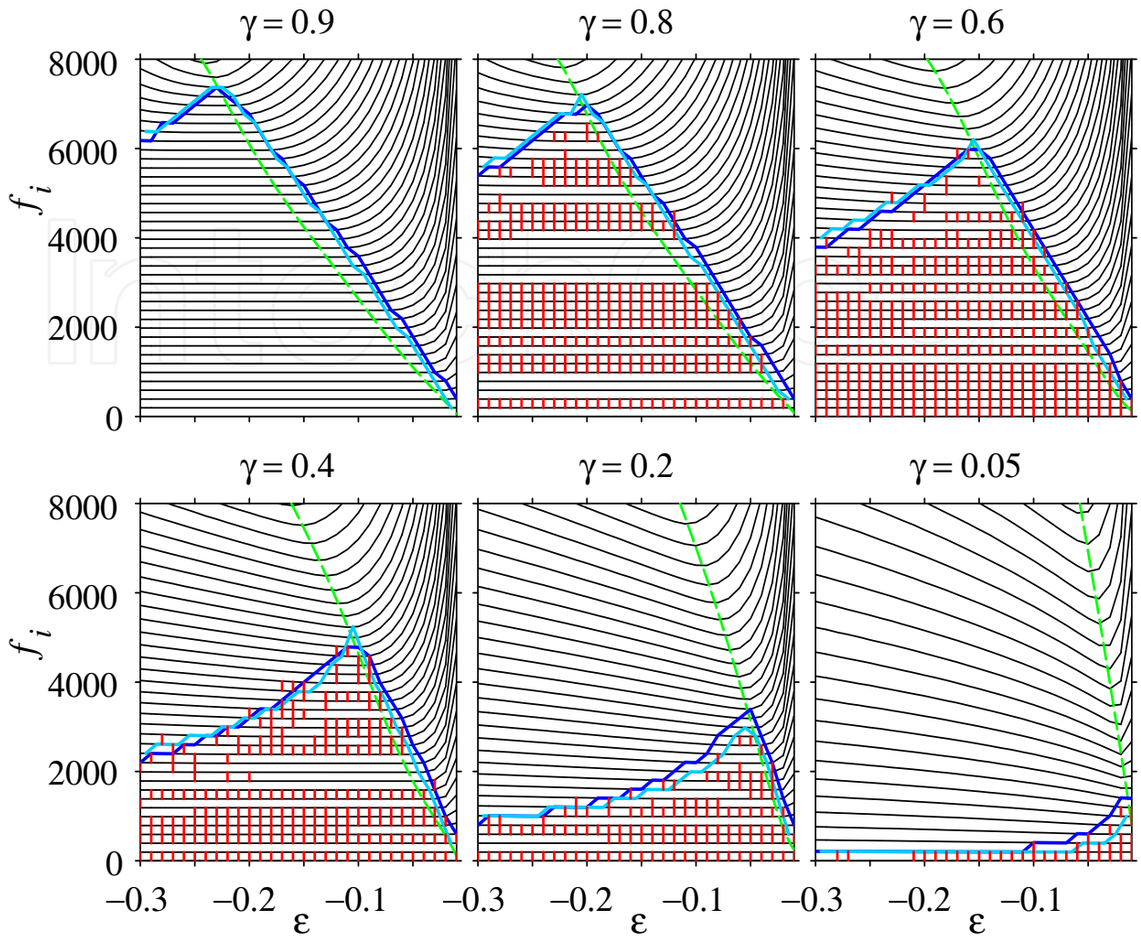

Fig. 1. Stretched level curves f_i at every 200 level along with the good domain on the $f_i - \epsilon$ plane. N_p =177, N = 7921, ℓ=even, m=0. Sky- and dark-blue mountain-like curves account for necessary conditions 1 and 2 respectively and the bulk under the curves satisfies sampling test (e.g. Fig. 2). In order to make curves, diagonalization is performed for each γ and for thirty values of scaling parameter ϵ ranging from -0.3 to -0.01 with inclement 0.01. The green dashed curve connects the minimum point of f_i and hits naturally the peak of the mountain. The level group with level-repulsion property is marked by red; these groups together remarkably overlap the domain for any γ (except the one $\gamma = 0.9 > 8/9$). For discussion on this, see subsection 3.1.

the following condition:

Condition 1: The level curves must be all horizontal. This is a necessary condition. In each diagram for respective γ the region under the (sky-blue) mountain-shaped curve is the *good ϵ-scaling region*.

One must consider one more condition. Recall that the spectrum (E_i) is stretched by Thomas-Fermi formula. If this procedure is valid the resultant spectrum (f_i) must satisfy $\delta f_i \approx 1$ apart from local fluctuations. Let us put this into a quantitative form;

Condition 2: The $|\langle \delta f_i \rangle_n - 1| \lesssim 0.05$.[6] Here n labels one of the 40 groups that the whole levels are divided into by ascending order. The region under the (dark-blue) mountain-shaped curve is the *successfully stretched region*. One observes a good overall agreement between two-types of regions, which gives a strong support for the celebrated WMB method. The bulk under the mountain-shaped curves in the $f_i - \epsilon$ plane in Fig. 1 is a candidate region for the study of level statistics satisfying both of necessary conditions. Let us call it the *good domain*.
Now we have to proceed a step forward; the energy levels are under subtle fluctuation and we must examine the level statistics (for each anisotropy γ) in order to understand the quantum AKP theory. Does the good domain maintain a unique level statistics?

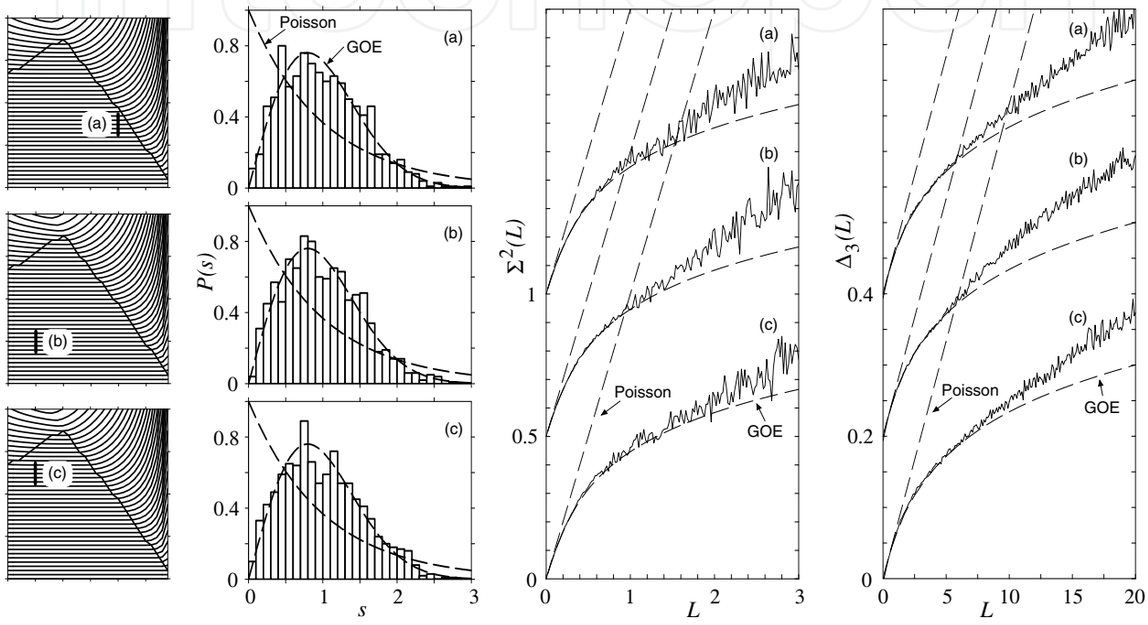

Fig. 2. Comparison of the level statistics $P(s)$, $\Sigma^2(L)$, $\Delta_3(L)$ sampled at regions (a), (b), (c). Note that graphs for the latter two statistics are properly shifted to avoid their overlap. The vertical axis is for (c).

Fig. 2 exhibits a sample of test. Here we have selected three regions (a, b, c), each consists of a thousand levels (5 groups) at a given ϵ. The comparison of the level statistics (Dyson, 1962; Dyson & Mehta, 1963; Mehta, 2004) in this figure succinctly shows that there is no sizable difference of the statistics with respect to any one of the three statistical characteristics; the spacing distribution $P(s)$, the number variance $\Sigma_2(L)$ and the spectral rigidity $\Delta_3(L)$. (For details of these quantities, see later discussion.) Repeating this test all over the good domain, we have checked that any region in the good main is equally satisfactory for the level statistics. Now we are in the position to propose a prescription to determine the proper ϵ for the eigenvalue analysis on the WMB method;

[6] We checked that the accepted region does not vary more than one group in height (200 levels) even if the bound is replaced by 0.1. On the other hand if the bound is decreased the region becomes sparse because of the tail of the $P(s)$ distribution. The averaging over the group acts to suppress this.

Prescription for ϵ: Choose the ϵ value that gives the maximum height of the good domain; then one can determine the largest number of levels at the given γ and at the given matrix size N. This ϵ is the best. We denote it ϵ^*.

2.2 Regularities regarding the best choice for ϵ

We have found the following empirical regularities regarding ϵ^*.

(i) Fig. 3 shows the relationship between γ and ϵ^*. Data points clearly follow a linear line described very well by

$$\epsilon^* \simeq (-1/4)\gamma. \tag{10}$$

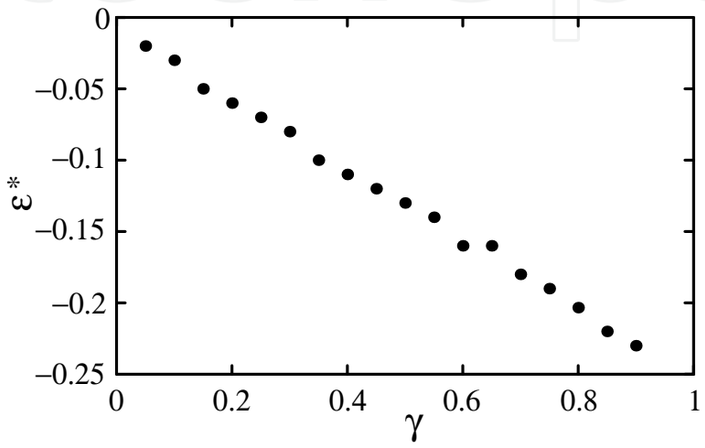

Fig. 3. The ϵ^* vs. γ.

(ii) Consider the ratio R_{eff} of the number of eigenvalues that satisfy conditions (1) and (2) to the number of whole levels N at ϵ^*. This is an indicator that tells us how much levels among all are really usable for the investigation of quantum level statistics. Fig. 4 shows plotted R_{eff} as a function of γ. We find it is described very well by

$$R_{eff} \simeq c\sqrt{\gamma}. \tag{11}$$

Here $c = 1$ with an error of only one per cent.

We have checked that these observations do not depend on the matrix size N. For instance, the small set $N = 1444(N_p = 75)$ shows the same features with the large set $N = 7921(N_p = 177)$. This independence assures the following planning of the AKP diagonalization using the WMB method. Using (10) as a rule of thumb, we can first easily estimate the appropriate ϵ^* that is appropriate for a given anisotropy γ. Then using (11), we can estimate the necessary matrix size N for obtaining desired number of energy levels. For instance, if one wants to examine the germanium (silicon) levels with $\gamma \approx 0.05$ (0.2), then $R_{eff} = 0.23$ (0.46) at $\epsilon^* = -0.01(-0.05)$. Then, to obtain first say 2000 reliable levels in the $\ell =$even and $m = 0$ sector, one has to choose $N \approx 8800(4400)$. On the other hand, for $\gamma = 0.8$, the appropriate ϵ^* now becomes -0.2 and

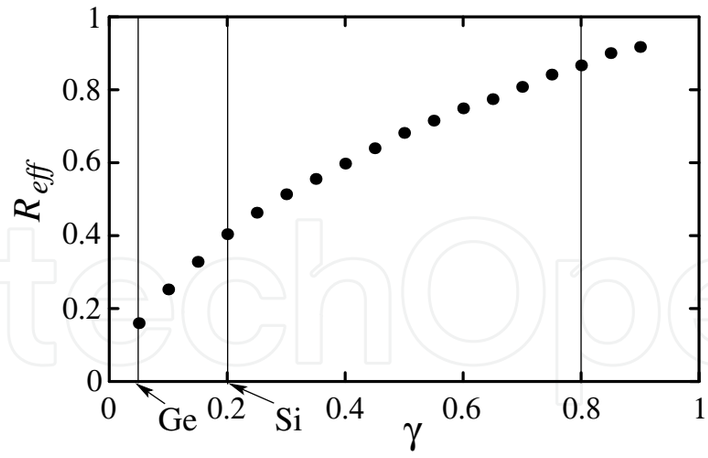

Fig. 4. Ratio of reliable levels vs. γ.

$R_{eff} = 0.9$. [7] Regularities (10) and (11) are remarkably simple. It is obvious that the ϵ^* curve in Fig. 3 starts from $\epsilon = -1/4$ at the Kepler limit ($\gamma = 1$) because, as we discussed below (7), the Sturmian basis is already the proper basis for the first order perturbation theory for AKP. This curve presumably represents the effect of truncating the basis in the WMB diagonalization. (10) and (11) are tantalizing.

2.3 Application of harmonic oscillator function basis to AKP

Harmonic oscillator function basis is quite useful for quantum chaos study through Husimi function (Husimi, 1940) and we discuss here the application of it to AKP. The formulation is almost parallel to that in subsection 2.1; main difference stems in the interaction terms. Let us introduce the semi-parabolic coordinates μ, ν, ϕ by

$$\mu\nu = \rho = \sqrt{x^2 + y^2},\ \frac{1}{2}(\mu^2 - \nu^2) = z,\ \phi = \tan^{-1}\left(\frac{y}{x}\right). \tag{12}$$

The AKP Schrödinger equation in terms of semi-parabolic coordinates is

$$\left[-\frac{1}{2(\mu^2+\nu^2)}\left(\Delta_\mu^{(2)} + \Delta_\nu^{(2)}\right) + \frac{1-\gamma}{2}\frac{\partial^2}{\partial z^2} - \frac{2}{\mu^2+\nu^2}\right]|\Psi\rangle = E|\Psi\rangle. \tag{13}$$

[7] The level statistics of AKP at $\gamma = 0.8$ were studied in the seminal paper (Wintgen & Marxer, 1988) but the choice of ϵ was not written there regrettably. Also no other data were published for other γ. In an earlier article (Wintgen et al., 1987) (the paper of WMB method), the low lying levels of silicon ($\gamma = 0.2079$) and germanium ($\gamma = 0.05134$) had been presented with the explicit statement of $\epsilon = -0.01$ for both cases. This led us to some confusion at the early stage of this work, because, for $\gamma = 0.8$, the proper choice is $\epsilon \approx -0.2$ much smaller than $\epsilon = -0.01$. Our level statistics results for $\gamma = 0.8$ agree with those in (Wintgen & Marxer, 1988) within errors; therefore we believe that ϵ was adjusted properly in (Wintgen & Marxer, 1988). We add that the best choice for Silicon is $\epsilon = -0.05$ rather than $\epsilon = -0.01$; this enhances R_{eff} approximately by factor 3. At these circumstances we revisited the whole level calculation and construct Fig. 1 (plus a dozen diagrams for other anisotropy).

Multiplying by $\mu^2+\nu^2$ and exchanging the Coulombic interaction term and the E term between the right and left hand sides, one obtains

$$\left[-\frac{1}{2}\left(\Delta_\mu^{(2)}+\Delta_\nu^{(2)}\right)+|E|(\mu^2+\nu^2)+\frac{1-\gamma}{2}(\mu^2+\nu^2)\frac{\partial^2}{\partial z^2}\right]|\Psi\rangle=2|\Psi\rangle. \tag{14}$$

Thanks to the semi-parabolic coordinates, the Coulombic singularity has removed (Kustaanheimo & Stiefel, 1965) (for $\gamma=1$).
One has now two of two-dimensional harmonic oscillators coupled by an interaction term $(\mu^2+\nu^2)\partial^2/\partial z^2$ introduced by the mass anisotropy in the original problem. Let us call the oscillators as $\mu-$ and $\nu-$ oscillators respectively. The proper basis for each oscillator is the harmonic oscillator basis and for two of them one uses tensor product of these bases. The $\mu-$ harmonic basis $\{|j,m\rangle\}$ is defined as eigenstates of the Schrödinger equation for the two-dimensional harmonic oscillator

$$\left(-\frac{1}{2}\Delta_\mu^{(2)}+\frac{1}{2}\mu^2\right)|j,m\rangle=(2j+1+|m|)\,|j,m\rangle \tag{15}$$

and the polar-coordinate representation of normalized $|j,m\rangle$ is given by

$$\begin{aligned}\langle\mu,\phi_\mu|j,m\rangle\equiv\psi_{jm}(\mu,\phi_\mu)&=\frac{1}{\sqrt{\pi}}\sqrt{\frac{j!}{(j+|m|)!}}e^{im\phi_\mu}L_j^{|m|}(\mu^2)e^{-\frac{\mu^2}{2}}\mu^{|m|},\\ \int_0^\infty\mu d\mu\int_0^{2\pi}d\phi_\mu\langle j',m'|\mu,\phi_\mu\rangle\langle\mu,\phi_\mu|j,m\rangle&=\delta_{jj'}\delta_{mm'}.\end{aligned} \tag{16}$$

For the $m=0$ sector of AKP, one should set $m_\mu=m_\nu=0$ and one uses tensor basis

$$\begin{aligned}|i,j\rangle&\equiv|i,m_\mu=0\rangle\otimes|j,m_\nu=0\rangle,\\ |\mu,\nu\rangle&\equiv|\mu,\phi_\mu=0\rangle\otimes|\nu,\phi_\nu=0\rangle,\\ \langle\mu,\nu|i,j\rangle\equiv\psi_{i0}(\mu)\psi_{j0}(\nu)&=\frac{1}{\pi}L_i(\mu^2)L_j(\nu^2)e^{-\frac{\mu^2+\nu^2}{2}}.\end{aligned} \tag{17}$$

In order to use WMB method let us modify basis $\{|i,j\rangle\}$ by introducing a scaling parameter κ. One replaces $\mu^2/2$ and $|j,m\rangle$ by $\kappa^2\mu^2/2$ and $|j,m,\kappa\rangle$. This leads to a modified basis $\{|i,j,\kappa\rangle\}$ with

$$\langle\mu,\nu|i,j;\kappa\rangle=\frac{\kappa}{\pi}L_i(\kappa\mu^2)L_j(\kappa\nu^2)e^{-\kappa\frac{\mu^2+\nu^2}{2}}. \tag{18}$$

With this basis (14) is written as the matrix equation

$$\begin{aligned}\sum_{i'',j''}\langle i',j';\kappa|\left\{-\frac{1}{2}\left(\Delta_{\mu(\mathrm{rad})}^{(2)}+\Delta_{\nu(\mathrm{rad})}^{(2)}\right)+|E|(\mu^2+\nu^2)+\frac{1-\gamma}{2}(\mu^2+\nu^2)\frac{\partial^2}{\partial z^2}\right\}\\ |i'',j'';\kappa\rangle\langle i'',j'';\kappa|\Psi\rangle=2\langle i',j';\kappa|\Psi\rangle.\end{aligned} \tag{19}$$

One finds

$$\langle i',j';\kappa|\mu^2|i,j;\kappa\rangle=\frac{1}{\kappa^3}\langle i',j';1|\mu^2|i,j;1\rangle \tag{20}$$

and corresponding scaling property of other terms are κ^{-2}, κ^{-1}, κ^{-1} for 1, $\Delta^{(2)}_{\mu(\mathrm{rad})}$, $(\mu^2+\nu^2)\partial^2/\partial z^2$ respectively. Using this scaling, (19) is transformed into

$$\sum_{i'',j''}\langle i',j';1|\left\{-\frac{1}{2}\left(\Delta^{(2)}_{\mu(\mathrm{rad})}+\Delta^{(2)}_{\nu(\mathrm{rad})}\right)+\frac{|E|}{\kappa^2}\left(\mu^2+\nu^2\right)+\frac{1-\gamma}{2}(\mu^2+\nu^2)\frac{\partial^2}{\partial z^2}\right\}|i'',j'';1\rangle$$

$$\times\langle i'',j'';\kappa|\Psi\rangle=\frac{2}{\kappa}\langle i',j';\kappa|\Psi\rangle. \quad (21)$$

The matrix elements for the first two terms are

$$\langle i',j';1|\left(\mu^2+\nu^2\right)|i,j;1\rangle=\Big[(2i+1)\delta_{i'i}\delta_{j'j}-(i+1)\delta_{i'i+1}\delta_{j'j}-i\delta_{i'i-1}\delta_{j'j}\Big]+\Big[i\leftrightarrow j\Big],$$

$$\langle i',j';1|\left(\Delta^{(2)}_{\mu(\mathrm{rad})}+\Delta^{(2)}_{\nu(\mathrm{rad})}\right)|i,j;1\rangle=(-1)^{i'+j'+i+j+1}\langle i',j';1|\left(\mu^2+\nu^2\right)|i,j;1\rangle. \quad (22)$$

Matrix elements of the third term [8] needs tedious but straightforward calculation [9].

$$\frac{1}{4}\mathcal{D}\frac{\partial^2}{\partial z^2}\langle\mu,\nu|i,j\rangle=\left\{-\left(\frac{1}{\mathcal{D}^2}+\frac{1}{\mathcal{D}}\right)\left((i-j)(\mu^2-\nu^2)+2\mu^2\nu^2\right)+\frac{\mu^2\nu^2-2ij}{\mathcal{D}}+\frac{1}{4}(\mu^2+\nu^2)\right\}\langle\mu,\nu|i,j\rangle$$
$$+\left[i\left(\frac{\mu^2-\nu^2}{\mathcal{D}^2}+\frac{2j-\nu^2}{\mathcal{D}}\right)\langle\mu,\nu|i-1,j\rangle\right]+\Big[\mu\leftrightarrow\nu,i\leftrightarrow j\Big]$$
$$-\frac{2ij}{\mathcal{D}}\langle\mu,\nu|i-1,j-1\rangle,\quad \mathcal{D}\equiv\mu^2+\nu^2=2r$$

and the necessary integration formula is

$$\int_0^\infty\mu d\mu\int_0^\infty\nu d\nu\,\frac{\mu^{2b}\nu^{2c}}{(\mu^2+\nu^2)^a}L_{n'}(\mu^2)L_n(\mu^2)L_{m'}(\nu^2)L_m(\nu^2)e^{-(\mu^2+\nu^2)},\quad (23)$$
$$(a\in\{0,1,2\},\ b\in\{0,1\},\ c\in\{0,1\}).$$

The case $a=0$ is straightforward; for $a=1,2$, one uses the integral of the type

$$L_n(\beta x)=\sum_{k=0}^{n}\binom{n}{k}\beta^k(1-\beta)^{n-k}L_k(x).$$

Now that we have obtained the matrix elements, our procedure goes parallel to that in subsection 2.1. Corresponding to (6) we introduce the parameter

$$\tilde{\epsilon}=2\frac{|E|}{\kappa^2}. \quad (24)$$

[8] For diamagnetic hydrogen case, the corresponding term is $B^2(\mu^4\nu^2+\mu^2\nu^4)$ (Müller & Wintgen, 1994) and easier to calculate.

[9] It can be useful to formulate with the creation and annihilation operators. Details will be discussed in our forthcoming paper.

Then one can solve (21) as the standard eigenvalue problem and can obtain eigenvalues $\Lambda_n = 2/\kappa_n$. Energy levels are determined by

$$E_n = -\frac{\kappa_n^2}{2}\tilde{\epsilon} = -\frac{2}{\Lambda_n^2}\tilde{\epsilon}. \tag{25}$$

It is found numerically that the best value of $\tilde{\epsilon}$ satisfies

$$\tilde{\epsilon}^* = \gamma \tag{26}$$

which is similar to (10). Finally we should add that we have found precise agreement between our calculations by the Sturmian basis and by the harmonic oscillator basis. [10]

3. Quantum level statistics in anisotropic kepler problem

3.1 Level repulsion

Let us first look at the nearest neighbor level spacing distribution $P(s)$ that is the probability for the nearest neighbor level appears at the distance $s\Delta$. Here Δ is the mean level spacing and after the stretch (9), $\Delta = 1$ in this subsection. First we recollect the RMT predictions. For γ near 1 the overlap of wave functions are negligible and $P(s)$ is expected to be Poisson. The mean squared deviation (MSD) of level spacings is then unity. On the other hand, for large anisotropy, the wave function overlap is sizable and quantum levels repel each other. Especially at the ergodic limit, the statistics is expected to be Wigner-Dyson(WD) statistics. Since AKP respects time reversal invariance, one expects the limiting level statistics is WD with $\beta = 1$ (GOE). (BGS conjecture). At this limit, the RMT prediction for the MSD of level spacing is as low as $4/\pi - 1 = 0.273\cdots$.

With this theoretical expectation in mind, let us first try a coarse analysis to obtain rough idea on where the level statistics is like WD distribution using data on $P(s)$. As the limiting MSD is 0.273, we set a condition $MSD \lesssim 0.28$. We indicate in Fig. 1 by vertical lines the regions where this condition is met. Here we observe that, except for $\gamma = 0.9$ (the first panel), whole of the region of reliable data (the region under the mountain) remarkably satisfy the condition, while other region does not. This indicates some consistency in our analysis. But, of course, looking only at the second moment is insufficient to tell the real shape of the distribution is like-WD.

Therefore, in order to step forward, we have calculated the $P(s)$ from our data extensively. In Fig. 5, we show real $P(s)$ distribution at $\gamma = 0.9,\ 0.8,\ 0.7$ as samples and compare with the prediction at limits (Poisson and GOE). We find that for $\gamma \lesssim 0.7$ the $P(s)$ is WD, and around $\gamma \sim 0.8$ a small deviation from WD starts. (But still satisfies above like-WD criterion). Now the $P(s)$ at $\gamma = 0.9$ is sizeably deviated from WD distribution. This explains why the like-WD criterion is not met at $\gamma = 0.9$. Furthermore, the deviation occurs mainly around $s = 1$ and remarkably the level repulsion still persists ($P(s) \propto s$). From this, it seems that AKP is not a system to have the Berry-Robnik distribution (Berry & Robnik, 1984) in which the $P(0)$ takes finite value depending on the partition of regular and chaotic orbits and rather a system that follows the stochastic approach (Hasegawa et al., 1988; Yukawa & Ishikawa,

[10] For instance, $E_{1800} = -0.00018114433$ and $E_{1800} = -0.00018114418$ for Sturmian and harmonic basis calculation respectively.

1989). The persisting repulsion at the transitive region reminiscent to the fact that, in the Anderson transition, not only in the metallic phase but also at the mobility edge the level repulsion occurs (Fyodorov & Mirlin, 1997). Noting that AKP is not a KAM system, it would be interesting to look at the change of the behavior of $P(s)$ near $\gamma = 1$ though it is difficult to apply proper stretch there.

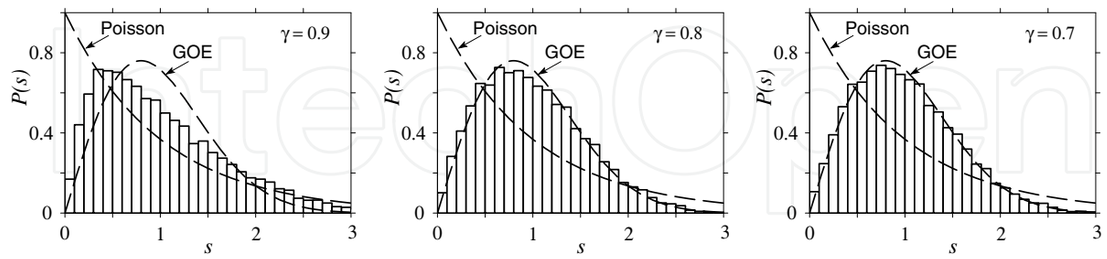

Fig. 5. Nearest neighbor level spacing distribution of AKP for $\gamma = 0.9, 0.8, 0.7$.

3.2 Level statistics as seen by $\Sigma^2(L)$ and $\Delta_3(L)$

As further statistical quantities one can consider the number variance $\Sigma^2(L)$ and the spectral rigidity $\Delta_3(L)$. These are both related to the level density-density correlation functions and suitable to the test for the RMT predictions. The number variance is defined as

$$\Sigma^2(L) = \left\langle (\hat{n}(L,E) - L)^2 \right\rangle \tag{27}$$

and the spectral rigidity [11] by

$$\Delta_3(L) = \left\langle \frac{1}{L} \min_{\{A,B\}} \int_{-L/2}^{L/2} \left(\hat{N}(E+x) - Ax - B\right)^2 dx \right\rangle. \tag{28}$$

Here $\hat{n}(L,E)$ is the number of (unfolded) levels within the band with L around E, $\hat{N}(E)$ is the stair case function, and $\langle \cdots \rangle$ implies the spectral average. Because both $\Sigma^2(L)$ and $\Delta_3(L)$ are derived from the two-point correlation functions, they are related by the Pandey relation (Pandey, 1979)

$$\Delta_3(L) = \frac{2}{L^4} \int_0^L (L^3 - 2rL^2 + r^3)\Sigma^2(r)dr. \tag{29}$$

This gives, for the Poisson statistics (independent levels), $\Delta_3(L) = L/15$ from $\Sigma^2(L) = L$. As a map from $\Sigma^2(L)$ to $\Delta_3(L)$, this gives enhanced weight for the low L side of $\Sigma^2(L)$.
In Fig. 6, we present for the first time the $\Sigma^2(L)$ and $\Delta_3(L)$ for various anisotropy ($\gamma = 0.85, 0.8, 0.7$). Prediction by RMT (GOE) is also shown;

$$\Sigma^2(L) = \frac{2}{\pi^2}\left[\log(2\pi L) + \gamma_E + 1 - \frac{\pi^2}{8}\right], \tag{30}$$

$$\Delta_3(L) = \frac{1}{\pi^2}\left[\log(2\pi L) + \gamma_E - \frac{5}{4} - \frac{\pi^2}{8}\right], \tag{31}$$

[11] $\Delta_3(L)$ was first introduced in (Dyson & Mehta, 1963) and studied in terms of the periodic orbit theory (Berry, 1985). The useful formulation for the numerical computation is found in (Bohigas & Giannoni, 1984).

for large L and in the small L region we give numerical estimate.
For $\gamma = 0.6$ and lower, the statistics become indistinguishable from the GOE.

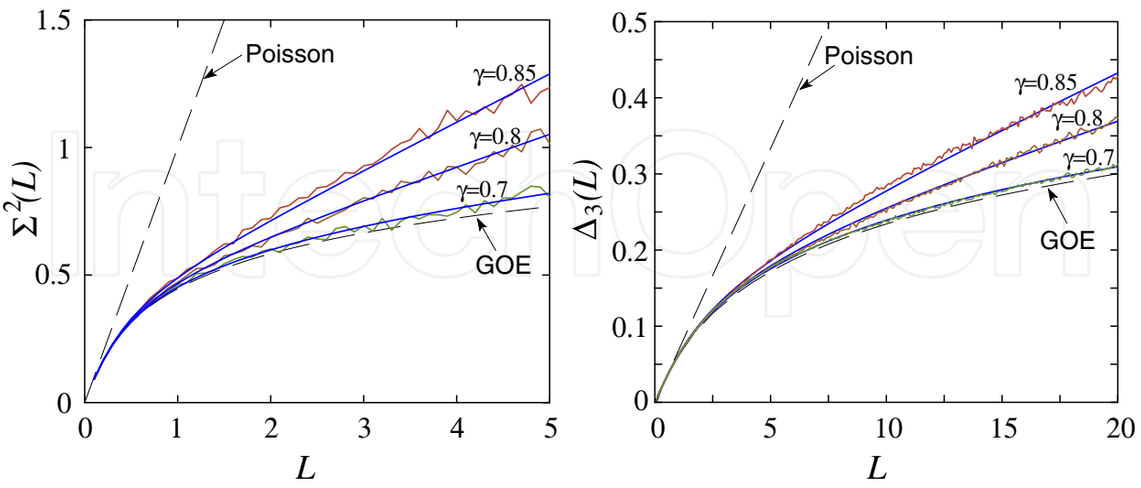

Fig. 6. Number variance $\Sigma^2(L)$ and spectral rigidity $\Delta_3(L)$) of AKP at $\gamma = 0.85, 0.8, 0.7$ calculated from 2501 to 12500 levels with $\ell =$ even, $m = 0$, $N = 19321(N_p = 277)$. The solid curves exhibits the prediction by the generalized GOE model (García-García & Verbaarschot, 2003) at $h = 0.160, 0.114, 0.034$ for $\Sigma^2(L)$ and $h = 0.178, 0.128, 0.032$ for $\Delta_3(L)$ respectively.

3.3 Critical random matrix theories

There is an important model by García-García & Verbaarschot (2003) (we call it GV model) of the critical level statistic for the T invariant system. It is an extension of the generalized GUE (Moshe et al., 1994) to generalized GOE. This extension is successfully performed by two threads of ideas; a map to the Calogero-Sutherland (CS) model (Calogero, 1969a;b; 1971; Sutherland, 1971a;b), which avoids the difficult integration over matrices in the GOE case, and the use of Kravtsov-Tsvelik (KT) conjecture for the density-density correlation function of the CS model in the low temperature limit (Kravtsov & Tsvelik, 2000).
The model is defined by the joint probability distribution

$$P(S,b) = \int dM e^{-\frac{1}{2}TrSS^T} e^{-\frac{b}{2}Tr[M,S][M,S]^T}, \tag{32}$$

where the matrices S and M are both $N \times N$ and real symmetric and orthogonal respectively. This is a one-parameter model; the parameter b interpolating two statistics. At $b \to 0$, the model becomes GOE ($P(S) \sim e^{-\frac{1}{2}TrSS^T}$). At $b \to \infty$, such S dominate that commute with arbitrary diagonal orthogonal matrices, i.e. the Poisson ensemble. The critical statistics is obtained if b is scaled as $b = h^2N^2$ for the large N limit.
The joint distribution of the eigenvalues $x \equiv (x_1, x_2, \cdots, x_N)$ of S is given by

$$\rho(x) = \Delta(x) \int dM e^{-\frac{2b+1}{2}TrS^2 + bTrSMSM^T} \tag{33}$$

where $\Delta(x) = \prod_{i<j}(x_i - x_j)$. Now, by considering the propagator of the matrix S in the imaginary time τ (Zirnbauer & Haldane, 1995), one obtains

$$\langle x|e^{-\tau\hat{H}_{CS;\lambda=1}}|x\rangle = C\int dM e^{-\frac{\omega}{2\sinh\omega\tau}\left[TrS^2\cosh\omega\tau - TrSMSM^T\right]} \tag{34}$$

where $\hat{H}_{CS;\lambda=1}$ in the left-hand side is the CS hamiltonian [12] with $\lambda = 1$. Therefore, by comparing (33) and (34), one finds that the joint eigenvalue distribution of GV model is given by the diagonal matrix elements of the N-particle density matrix of CS model at an inverse temperature τ given by the identification $\omega/\sinh\omega\tau = 2b$, $\omega\cosh\omega\tau/\sinh\omega\tau = 2b+1$.
The KT conjecture gives the low temperature limit of connected density-density correlation function of CS model at $\lambda = 1$ as

$$R^T_{2,c}(x,0) = -(\overline{K}_T(x,0))^2 - \left(\frac{d}{dx}\overline{K}_T(x,0)\right)\int_x^\infty \overline{K}_T(t,0)dt \tag{36}$$

where $\overline{K}_T(x,0) = T\sin(\pi x)/\sinh(\pi xT)$ is the kernel of CS model for $\lambda = 2$ and $T = \pi h/2$. (García-García & Verbaarschot, 2003) suggests to replace it by its finite temperature analog (Moshe et al., 1994) and then the unfolded spectral kernel is given by [13]

$$\overline{K}^T(x,0) = \sqrt{h}\int_0^\infty \frac{\cos(\pi x\sqrt{ht})}{2\sqrt{t}}\frac{1}{1+z^{-1}e^t}dt. \tag{37}$$

From the density-density correlation function (36) with (37) one can calculate $\Sigma^2(L)$ by

$$\Sigma^2(L) = L + 2\int_0^{L/\rho(0)} ds(L-s)R^{T=\pi h/2}_{2,c}(s,0) \tag{38}$$

and the spectral rigidity $\Delta_3(L)$ through the Pandey relation (29). The above summarizes the work by García-García & Verbaarschot (2003).
Now we are in a position to compare their predictions with the AKP data with respect to the variation of γ. We have verified, first of all, the AKP data of $\Sigma^2(L)$ and $\Delta_3(L)$ satisfy the Pandey relation in order to guarantee that AKP levels are normal statistical set (Pandey, 1979). Now in order to test that the GV model can explain $\Sigma^2(L)$ and $\Delta_3(L)$ coherently, we have performed a one parameter fit, at each γ, for the best h that explains $\Sigma^2(L)$ data and $\Delta_3(L)$ data independently. Since the $\Sigma^2(L)$ soon shows large fluctuation for large L, we have limited to $L \lesssim 5$ for the $\Sigma^2(L)$ fit, and used $L \lesssim 20$ for the $\Delta_3(L)$ fit. The level set we used is the largest one that is obtained by the diagonalization of 19321×19321 ($N_p = 277$) hamiltonian matrix (at each γ) and we used the reliable 10^4 levels starting from 2501-th.
The result exhibited in Fig. 7 succinctly shows that the GV model well describes the AKP data in the range of γ from 0.75 up to 0.9. The discrepancy between the $\Sigma^2(L)$ fit and $\Delta_3(L)$ fit is

[12] The CS hamiltonian is

$$\hat{H}_{CS} = -\sum_j \frac{\partial^2}{\partial x_j^2} + \frac{\lambda}{2}\left(\frac{\lambda}{2}-1\right)\sum_{i\neq j}\frac{1}{(x_i-x_j)^2} + \frac{\omega^2}{4}\sum_j x_j^2. \tag{35}$$

[13] A typographical error in equation (30) of García-García & Verbaarschot (2003) is corrected in their arXiv:cond-mat/0204151(version 2) and we have corrected for it in (37).

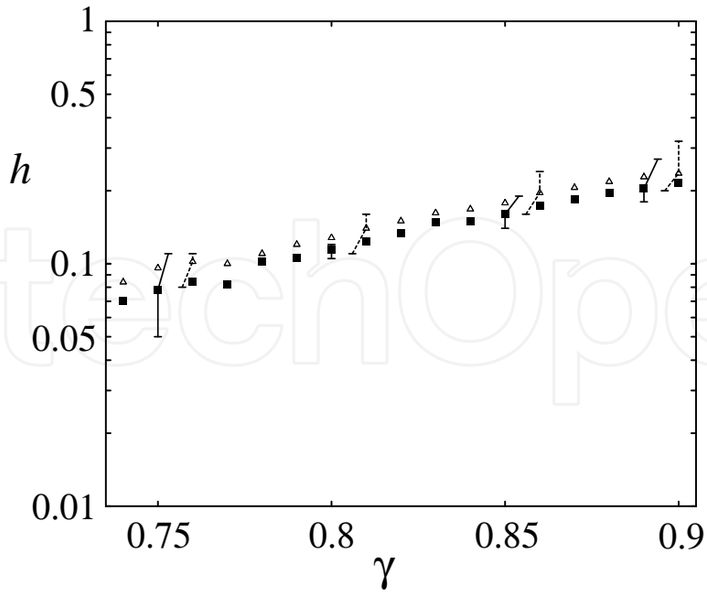

Fig. 7. The parameter h in the critical random matrix model (García-García & Verbaarschot, 2003) as determined by number variance (box with solid error bar) and by spectral rigidity (triangle with dashed error bar).

negligible. The parameter h is related to the temperature T of the CS model as $T = \pi h/2$. We note that the correspondence between h and anisotropy γ is well described by a simple approximation

$$h \propto e^{7.2\gamma}. \tag{39}$$

In the physics of Anderson transition, a finite size scaling analysis turns out vital to scrutinize the phase transition point (García-García & Wang, 2008; Shklovskii et al., 1993). In order to compare with it, we are now trying a similar analysis using our results at various sizes. So much for the eigenvalues. Now let us turn to the wave functions.

4. Wave function features in anisotropic kepler problem

Here we describe three important features of AKP wave functions. Firstly, we show the systematic increase of the complexity of wave function nodal lines ($\{\mathbf{r}|\Psi_i(\mathbf{r}) = 0\}$) with the increase of the anisotropy $1-\gamma$. Secondly, the probability density $|\Psi_i(\mathbf{r})|^2$ is investigated and it is shown that salient scars of periodic orbits are observed. Thirdly, we describe the method to evaluate Husimi functions using the basis given in subsection 2.3 and compare the Husimi distributions with the Poincaré section of the above scarring periodic orbits.

4.1 Nodal lines of AKP wave functions

The systematics of nodal lines of the eigenfunction of the laplacian operator has long history. For instance, we can find an amazing example in (Courant&Hilbert, 1953) of a self-avoiding long nodal line of an eigenfunction of a laplacian, that propagates in the whole rectangle only by itself (Fig. 8).

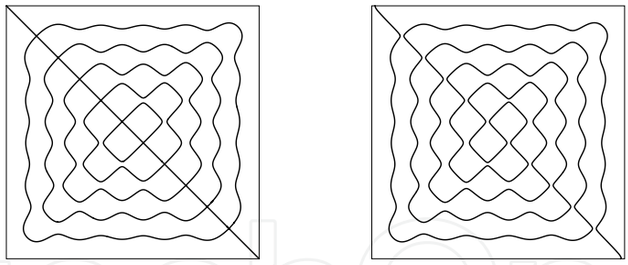

Fig. 8. The nodal line of an eigenfunction $u(x,y) = \sin(2rx)\sin y + \mu \sin x \sin(2ry)$ of an eigenvalue problem $\Delta u + \lambda u = 0$ in the square region $S \equiv [0,\pi]^2$ with Dirichlet boundary condition $u|_{\partial S} = 0$ with eigenvalue $\lambda = 1 + 4r^2$. Left: $\mu = 1$ and right: $\mu = 0.96$. $r = 6$ is chosen to reproduce the figures in (Courant&Hilbert, 1953).

In general, the nodal line for the wave function in the non integrable case is self-avoiding. At the would be crossing, the function must be zero, and also it must be a saddle point. Both conditions can be met only coincidentally. We refer to (Gutzwiller, 1990) for nodal lines. Also we refer to a recent interesting example, the nodal line of the Maass wave form on modular surface $PSL(2,Z) \setminus H$ calculated by (Hejhal & Rackner, 1992) and the increase of the complexity at higher eigenvalues.
In Fig. 9 we exhibit the nodal line of AKP wave function $\Psi_{438}(\mathbf{r})$ at $\gamma = 1, 0.95, 0.8, 0.2$. [14] One observes that even a small anisotropy, the crossings of nodal lines at the integrable limit ($\gamma = 1$) are resolved. With increasing anisotropy, nodal loops are created, and nodal lines increase their complexity. In the ergodic region ($\gamma = 0.2$), nodal lines become very complex. It seems that nodal lines in the large anisotropy region show some fractal structure. (Compare the right magnified diagram with the left one at $\gamma = 0.2$.) We are pursuing this issue introducing manifold with smoothened Coulomb singularity. The relation between the multi-fractality of wave functions (see section 5) is also under survey.

4.2 Large value of wave functions and periodic orbits

Let us try a straight forward comparison between the probability distribution of the AKP electron predicted by the wave function and periodic orbits. We have constructed and scanned $|\Psi_i(\mathbf{r})|^2$ for all of the wave functions up to some 5000-th level for anisotropy γ from 0.05 to 0.98. For intermediate γ ($0.85 - 0.5$), the pattern varies level by level almost randomly, but we observe that there are recognizably characteristic patterns (around ten or so) that appear repeatedly. If we pick one level at random, and calculate its $|\Psi(\mathbf{r})|^2$, the pattern is similar to one of the characteristic patterns or a combination of a few of them. On the other hand, for higher anisotropy $\gamma < 0.5$, the probability pattern becomes so complex that we cannot identify characteristic pattern.
In Fig. 10, we exhibit two of characteristic patterns at $\gamma = 0.6$, $|\Psi_{438}|^2$ and $|\Psi_{579}|^2$ on the μ-ν plane. We have already stored periodic orbits by increasing order of the Bernoulli coding up to 8 binary digits. (For this task we benefited from a paper (Gutzwiller, 1981) which gives classification of AKP periodic orbits considering time-reversal and symmetries around axes.) In the figure selected periodic orbits that run on the μ-ν plane along the large value region

[14] The choice of the energy is just to guarantee the visibility of the nodal line. One could choose equally $\Psi_{12500}(\mathbf{r})$ and the calculation of nodal lines is equally possible.

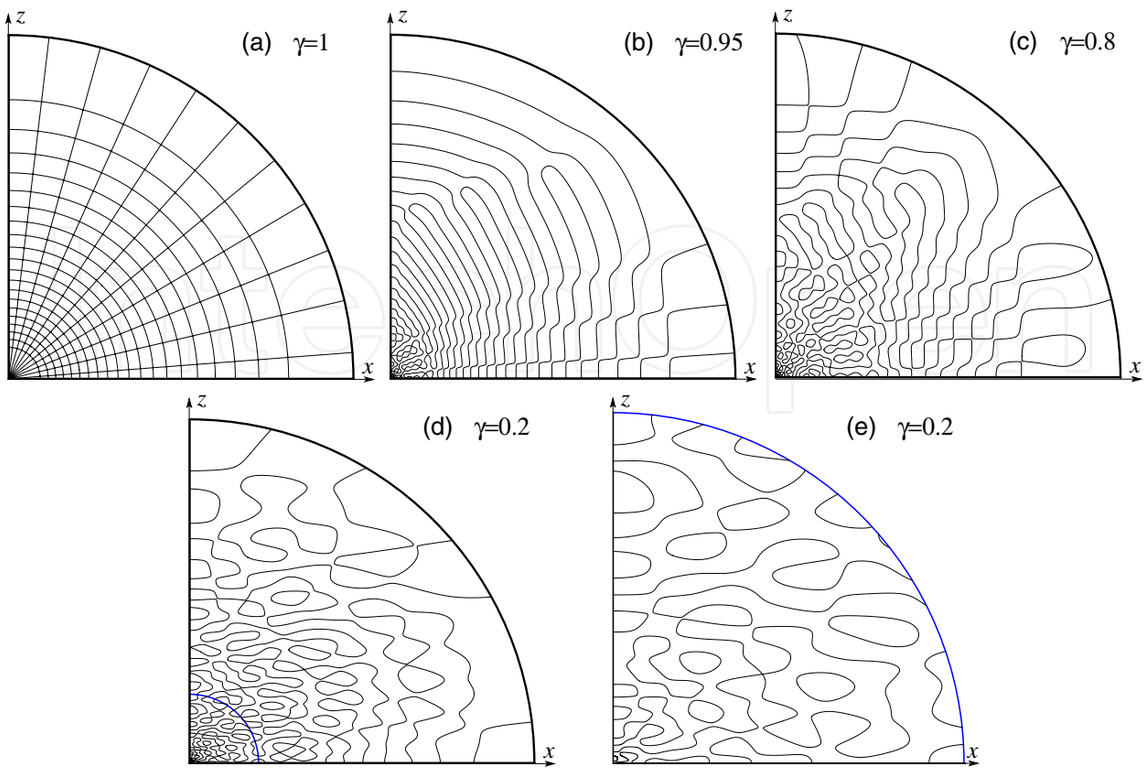

Fig. 9. Nodal lines of the AKP wave function $\Psi_i(\mathbf{r})$ with $i = 438$ in the sector $\ell =$ even, $m = 0$ in the $x - z$ plane. (z axis, vertical, is the heavy axis). $\gamma = 1,\ 0.95, 0.8, 0.2$ for (a), (b),(c), [(d), (e)] respectively. The energies are approximately equal for all, and for the integrable case (a) $\Psi_{n_p=41,\ell=20,m=0}(\mathbf{r})$ is chosen among the degenerate levels. Two diagram are shown for $\gamma = 0.2$. The right is a magnified plot of $r \leq 0.2$ part of the left one.

of the probability distribution are also exhibited. These are the *scarring orbits* in the sense of (Heller, 1984; 1989). It seems that the association of one periodic orbit(PO) to one probability distribution is *not* ad hoc, since with the change of γ, both PO and large value region change keeping the association. This observation takes the advantage of one-parameter characteristic of AKP and we are consolidating this.

4.3 Husimi function and Poincaré surface of section

Husimi function for $|\Psi_n\rangle$ is

$$W^{Hus}_{\Psi_n}(\boldsymbol{q}_0, \boldsymbol{p}_0) = |\langle CHS|\Psi_n\rangle|^2 = \left|\sum_{i,j}\langle CHS|i,j;\kappa_n\rangle\langle i,j;\kappa_n|\Psi_n\rangle\right|^2 . \tag{40}$$

Here $|CHS\rangle$ denotes the coherent state, a Gaussian packet centered at $(\boldsymbol{q}_0, \boldsymbol{p}_0)$ and width b

$$\langle \boldsymbol{q}|CHS\rangle = \frac{1}{\sqrt{\pi}b} e^{i\boldsymbol{p}_0\cdot\boldsymbol{q} - \frac{(\boldsymbol{q}_0-\boldsymbol{q})^2}{2b^2}} . \tag{41}$$

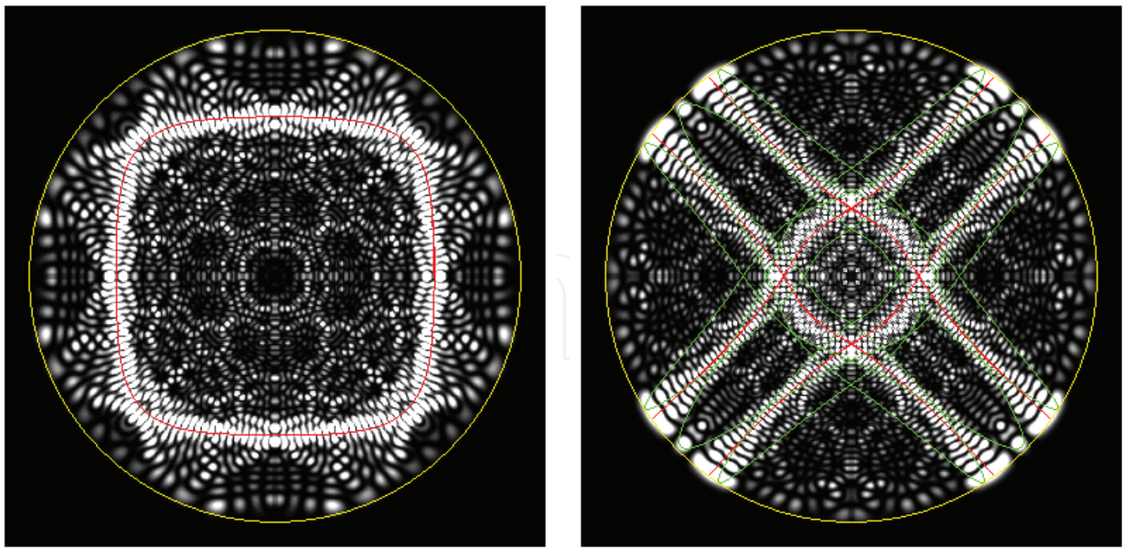

Fig. 10. AKP probability distributions in the $\mu - \nu$ plane. $\gamma = 0.6$, $m = 0$, $\ell =$even. Left: $|\Psi_{438}(\mathbf{r})|^2$. Right: $|\Psi_{579}(\mathbf{r})|^2$. Scarring short periodic orbits are also exhibited. Left: the primary periodic orbit $(+-)$. Right: $(++--)$ and $(++-+--)$ exhibited by red and green respectively. Surrounding yellow circle shows the boundary of the classical motion.

Following (Müller & Wintgen, 1994) we obtain

$$\begin{aligned} |CHS\rangle &= |I_\mu, \eta_\mu\rangle_b \otimes |I_\nu, \eta_\nu\rangle_b \\ &= \frac{1}{\sqrt{\mathcal{I}_0(I_\mu)\mathcal{I}_0(I_\nu)}} \sum_{j,k=0}^{\infty} (-1)^{j+k} \left(\frac{I_\mu}{2}\right)^j \left(\frac{I_\nu}{2}\right)^k \frac{e^{2i(j\eta_\mu + k\eta_\nu)}}{j!k!} |j,k;1/b^2\rangle \end{aligned} \tag{42}$$

where $|j,k;1/b^2\rangle$ is given by (18) with $\kappa = 1/b^2$. In Fig. 11 we exhibit the Husimi function of Ψ_{438} and Ψ_{579} on the μ-p_μ plane. (The same wave functions with Fig. 10). We observe that the Poincaré section of periodic orbits that are associated with the large probability distributions in Fig. 10 (the scarring orbits) is now clearly sitting in the midst of the large value region of Husimi function (creating scars). It is interesting to note that the fundamental periodic orbit which creates a strong scar in Ψ_{438} seems to be creating an anti-scar in Ψ_{579} and the same contrast holds for other two PO's too. We finally mention that the patterns in Fig. 11 are remarkably reminiscent of the classical phase space structure presented in Fig. 1 of the seminal paper (Wintgen & Marxer, 1988). We are now extensively studying the correspondence between the quantum and classical phase space structures.

5. Future outlook

We discuss here two of currently pursuing problems.

5.1 Physics of quantum chaos and Anderson localization

For one thing, we contemplate to investigate the relation of quantum chaos to the Anderson localization — a very extensively studied branch of quantum physics (see for instance, Evers & Mirlin (2008)). The multi-fractality of AKP wave function was conjectured by (García-García

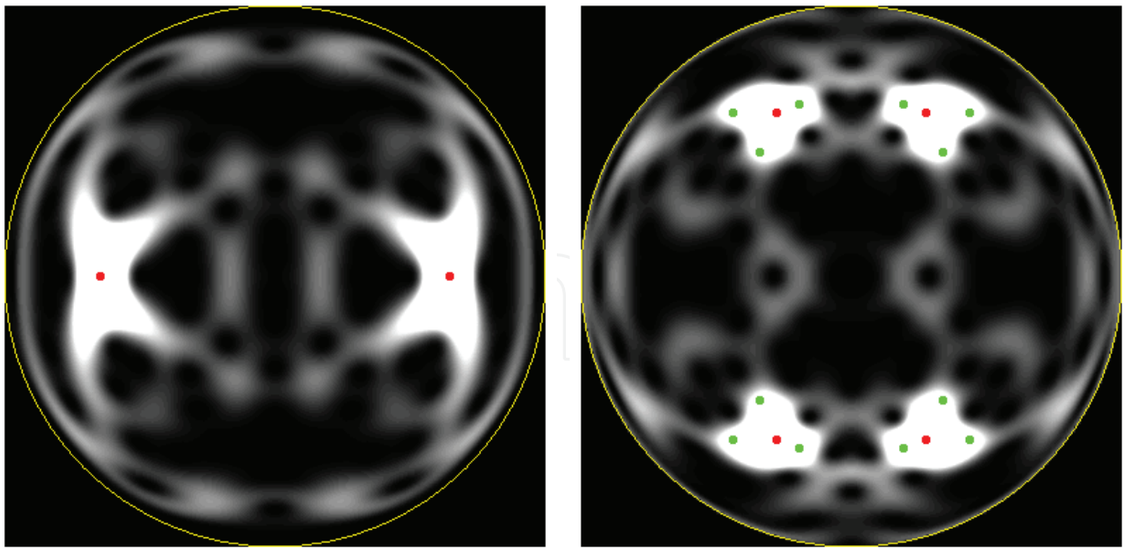

Fig. 11. Husimi function at Poincaré surface of section defined by $\nu = 0$ for Left:$\Psi_{438}(\mathbf{r})$ and Right:$\Psi_{579}(\mathbf{r})$. $\gamma = 0.6$, $m = 0$, ℓ =even. White regions indicate large value. The Poincaré shots of scarring short periodic orbits in Fig. 10 are superposed. Surrounding yellow circle shows the boundary of the classical motion.

& Verbaarschot, 2003) and AKP was considered as a candidate system to test an interesting scheme *Anderson transition in quantum chaos* by (García-García, 2007).
The general picture of Anderson localization is as follows (Fyodorov & Mirlin, 1997). At the metallic phase, a typical wave function is extended, the overlap of wave functions of nearby energy levels leads to the repulsion, and the statistics is WD. Approaching the Anderson transition point E_c, the wave functions show up multi-fractal structure. The level statistics deviates from WD, but remarkably the repulsion still persists, which is an intrinsic feature of quantum dynamics of Anderson localization. The statistics at the transition point (the mobility edge), the critical level statistics, is just between WD and Poisson. Passing the transition point into the insulator side, the wave functions become well localized, the overlap is negligible, and the level statistics is Poisson.
Now we have seen, in the quantum chaos study of AKP, a very similar phenomenon (see Table 1).

Anderson localization	level statistics	quantum chaos (AKP)	classical AKP
insulator	Poisson	$\gamma \lesssim 1$	(decaying tori?)
Mobility Edge	critical statistics	$0.75 \lesssim \gamma \lesssim 0.85$	Cantori (Web of chaos)
metal	Wigner-Dyson	$\gamma \lesssim 0.6$	isolated unstable P. O.s

Table 1. Anderson localization and quantum chaos (AKP).

In order to consolidate this correspondence, a crucial test would be the verification of the multi-fractality of wave function in AKP in the region of critical level statistics.
The multi-fractal nature of the wave function at the mobility edge is reflected in the *compressibility* of the energy levels as seen as the one-dimensional gas

$$\Sigma^2(L) = \chi L \quad (L \gg 1) \tag{43}$$

where χ is a constant less than one. (For Poisson statistics, $\Sigma^2(L) = L$ and $\chi = 1$, while for WD statistics, $\Sigma^2(L) = c\log(L)$ and $\chi = 0$, see (30)). The value of χ is exactly expressed by a formula derived by Chalker et al. (1996a)

$$\chi = \frac{d - D_2}{2d} \tag{44}$$

where d is the system dimension and the multi-fractal dimension D_2 necessary for the $R_2(s)$ statistics quantity $\Sigma^2(L)$ is defined by

$$\left\langle \int d^d r |\psi_n(r)|^{2p} \right\rangle \propto L^{-D_p(p-1)} \tag{45}$$

with $p = 2$. As this is a key formula relating the level statistics and the wave function structure, let us briefly follow (Chalker et al., 1996a;b) for its derivation. The compressibility χ can be calculated from the spectral form factor $K(t)$ (the Fourier transform of the two level correlation function $R(s)$, $K(t) = \int_{-\infty}^{\infty} ds e^{-ist/t_H} R(s)$ with the Heisenberg time t_H [15]) by taking a limit (Aronov et al., 1994; Kravtsov et al., 1994)

$$\chi = \int_{-\infty}^{\infty} R(s)ds \equiv \lim_{t\to 0} K(t). \tag{46}$$

Then there is a deep formula

$$K(t) = \frac{1}{2} \frac{|t| p(t)}{\pi\hbar\rho + \int_{0^+}^{|t|} p(t')dt'} \tag{47}$$

that gives the spectral form factor $K(t)$ by the return probability $p(t)$. It is introduced as a probability for the wave packet originally created in a small volume $V_0 = \ell^d$ to remain within this volume at time t

$$p(t) = \int d^d r \left\langle \sum_{k<\mathcal{N}_0} |\psi_n(r)|^2 |\psi_{n+k}(r)|^2 \, e^{-i\frac{(E_n - E_{n+k})t}{\hbar}} \right\rangle \tag{48}$$

with $\mathcal{N}_0 \sim L^d/V_0$. At this point the physics of energy levels meet the physics of eigenfunctions. The return probability should behave as

$$p(t) \sim V_0^{D_2/d-1} \left(\frac{\hbar\rho}{t}\right)^{D_2/d} \tag{49}$$

at the mobility edge (Chalker & Daniell, 1988; Chalker, 1990; Huckestein & Schweitzer, 1994). Now, inserting (49) into (47) and noting that the first term in the denominator is negligible compared with the second term

$$\pi\hbar\rho \Big/ \int_{0^+}^{|t|} p(t')dt' \propto \frac{1}{L^d} \left(\frac{t_H}{t}\right) t^{\frac{D_2}{d}} \to 0 \tag{50}$$

[15] The Heisenberg time t_H is defined by $t_H = \hbar/\Delta$ and Δ is the mean level spacing $\Delta = 1/(\langle\rho\rangle L^d)$ with the system size L.

for $t \ll t_H$ and at $L \to \infty$, one ultimately obtains (44).
Coming back to AKP, we have seen already that the $\Sigma^2(L)$ for large L is linearly rising in the critical statistics region. Based on this observation (and with further support of kicked particle) García-García and Verbaarschot (García-García & Verbaarschot, 2003) conjectured the multi-fractal structure of AKP wave functions in this region. We are currently working to verify quantitatively this conjecture based on (49) by our AKP data. Once the comparison of Table 1 is established, it would also give a supporting contribution to the extremely ambitious theme *Anderson localization in quantum chaos* by García-García & Wang (2008).

5.2 A non-trivial test of periodic orbit theory in AKP

Our another concern is to understand the spectral rigidity $\Delta_3(L)$ of AKP from the periodic orbit theory following the seminal paper by (Berry, 1985). In terms of periodic orbits, the behavior of $\Delta_3(L)$ for $L \ll L_{max}$ is predicted universally by the contribution of very long classical orbits under the sum rule by (Hannay & Ozorio de Almeida, 1984). [16] On the other hand, using a semi-classical sum rule, it is shown that the behavior of $\Delta_3(L)$ for $L \gg L_{max}$ is non-universally determined by the short periodic orbits. More precisely, it is of order $\hbar^{-(N-1)}$ for integrable models, and $\log(\hbar^{-1})$ for chaotic systems; the discrepancy comes from the manner of quantum interference. As we have described in the introduction, the isolated unstable orbits in AKP is symbolically coded by binary digits (Bernoulli sequences) and there is an amazing formula found by (Gutzwiller, 1980; 1981) that gives a good estimate of the action for each periodic orbits concisely and enables one to evaluate the contribution of whole periodic orbits. We have already checked, using our $\Delta_3(L)$ data, that the above L_{max} seems to give a right value for the change of $\Delta_3(L)$ from logarithmic rise to the asymptotic plateau. We are now trying to explain the plateau values of $\Delta_3(L)$ data for various γ from the contribution of short periodic orbits of AKP.

6. Conclusion

AKP is an old working ground which produced fruitful results on quantum chaos, especially via the pioneering works by Gutzwiller (Gutzwiller, 1971; 1977; 1980; 1981; 1982; 1990), and via the work by Wintgen (Wintgen & Marxer, 1988). It seems however that the focus of quantum chaos study has been shifted to elsewhere though for us it seems many things are still waiting for clarification in AKP. In this article we have extensively revisited AKP and have shed lights on its quantum features from the critical random matrix theories and from the insights from Anderson transition theories. We have in particular devoted ourselves to the quantitative investigation how the anisotropy in AKP affects systematically the quantum features of AKP. To this end, we have calculated quantum levels and wave functions from scratch. In section 2, we have recapitulated the vital WMB method (Wintgen et al., 1987) for the quantum levels. This method includes a key parameter ϵ and the effect in the eigenvalue calculation is exhibited in Fig. 1. Based on it, we have presented a prescription how to select the best ϵ for a given γ, and we have given simple rules (Fig. 3, 4). Besides the original WMB in AKP using the Sturmian basis, we have also formulated WMB calculation of AKP in terms of tensored harmonic basis. This in one hand provides us with a precise check of eigenvalues, and on the other hand, with necessary data for the Husimi function calculation. In section 3,

[16] $L_{max} \sim \hbar^{-(N-1)}$ for a system of N freedoms.

we have investigated the energy level statistics and have shown that GV model (García-García & Verbaarschot, 2003) successfully describes the statistics in a range $0.75 \lesssim \gamma \lesssim 0.9$. The finite scaling property is under survey. We have furthermore obtained a simple rule $h \propto e^{7.2\gamma}$ that relates the effective temperature in the CS model (equivalent to GV random matrix model) to the AKP anisotropy. In section 4 we have investigated the wave functions and Husimi functions. In both, salient quantum scar of classical unstable periodic orbits are observed. We have found that the nodal line of the wave function (at given energy) increases its complexity and seems to extend a fractal structure. In section 5 we have discussed our current projects, one on the multi-fractality of wave functions that may be deeply related to the Anderson localization, and the other on the non-trivial test of the periodic orbit theory in terms of the finite non-universal asymptote in $\Delta_3(L)$.

Acknowledgement:
K. K. thanks the post doctoral fellowship from Meiji University, Japan. Both of us thank Professor M. C. Gutzwiller for kindly replying to our letter and also referring us to a stimulating paper (Gutzwiller, 1981).

7. References

Aronov, A. G., Kravtsov, V. E. & Lerner, I. V. (1994). Spectral correlations in disordered electronic systems: Crossover from metal to insulator regime, *Physical Review Letters* 74: 1174-1177.

Berry, M. V. (1985). Semiclassical theory of spectral rigidity, *Proceedings of Royal Society London* 400: 229-251.

Berry, M. V. & Robnik, M. (1984). Semiclassical level spacings when regular and chaotic orbits coexist, *Journal of Physics* A17: 2413-2421.

Bohigas, O., Giannoni, M. J. & Schmit, C. (1984). Characterization of chaotic quantum spectra and universality of level fluctuation laws, *Physical Review Letters* 52: 1-4.

Bohigas, O. & Giannoni, M. J. (1984). Chaotic motion and random matrix theories, *in* Dehesa, J. S., Gomez, J. M. G. & Polls, A. (ed.), *Mathematical and Computational Methods in Nuclear Physics, Lecture Notes in Physics Vol. 209*, Springer-Verlag, Berlin, pp. 1-99.

Bohigas, O. (2005). Quantum chaos, *Nuclear Physics* A 751: 343c-372c.

Calogero, F. (1969a). Solution of a three-body problem in one dimension, *Journal of Mathematical Physics* 10: 2191-2196.

Calogero, F. (1969b). Ground state of a one-dimensional *N*-body system, *Journal of Mathematical Physics* 10: 2197-2200.

Calogero, F. (1971). Solution of the one-dimensional *N*-body problems with quadratic and/or inversely quadratic pair potentials, *Journal of Mathematical Physics* 12: 419-436.

Chalker, J. T. & Daniell, G. J. (1988). Scaling, diffusion, and the integer quantized hall effect, *Physical Review Letters* 61: 593-596.

Chalker, J. T. (1990). Scaling and eigenfunction correlations near a mobility edge, *Physica* A167: 253-258.

Chalker, J. T., Kravtsov, V. E. & Lerner, I. V. (1996a). Spectral rigidity and eigenfunction correlations at the Anderson transition, *Journal of Experimental and Theoretical Physics Letters* 64: 386-392.

Chalker, J. T., Lerner, I. V. & Smith, R. A. (1996b). Random walks through the ensemble: Linking spectral statistics with wave-function correlations in disordered metals,

Physical Review Letters 77: 554-557; Fictitious level dynamics: A novel approach to spectral statistics in disordered conductors, *Journal of Mathematical Physics* 37: 5061-5086.

Chaudhury, S., Smith, A., Anderson, B. E., Ghose, S.&Jessen, P. S. (2009). Quantum signatures of chaos in a kicked top, *Nature* 461; 768.

Courant, R.& Hilbert, D. (1953) *Methods of mathematical physics I*, Interscience Publishers, Inc.. See Fig. 7, 8 in Sec. 6 of Chap.6. (It is written that $r = 12$, but we consider it is a simple typographical error of $r = 6$.) The authors refer to the work by A. Stern (Bemerkungen über asymptotisches Verhaltan von Eigenwerten und Eigenfunktionen, Dissertation, Göttingen,1925).

Dyson, F. J. (1962). Statistical theory of the energy levels of complex systems. I, II, III, *Journal of Mathematical Physics* 3: 140-156, 157-165, 166-175.

Dyson, F. J. & Mehta, M. L. (1963). Statistical theory of the energy levels of complex systems. IV, *Journal of Mathematical Physics* 4: 701-712.

Mehta, M. L. & Dyson, F. J. (1963). Statistical theory of the energy levels of complex systems. V, *Journal of Mathematical Physics* 4: 713-719.

Evers, F. & Mirlin, A. D. (2008). Anderson transitions, *Review of Modern Physics* **80**: 1355-1417.

Fyodorov, Y. V. & Mirlin, A. D. (1997). Strong eigenfunction correlations near the Anderson-localization transition, *Physical Review* B 55: R16001-R16004.

García-García, A. M. & Verbaarschot, J. J. M. (2003). Critical statistics in quantum chaos and Calogero-Sutherland model at finite temperature, *Physical Review* E 67: 046104-1 - 046104-13.

García-García, A. M. (2007). Universality in quantum chaos and the one parameter scaling theory (a power point of a talk).
http://www.tcm.phy.cam.ac.uk/ amg73/oslo2007.ppt.

García-García, A. M. & Wang, J. (2008). Universality in quantum chaos and the one-parameter scaling theory, *Physical Review Letters* 100: 070603-1 - 070603-4.

Gutzwiller, M. C. (1971). Periodic orbits and classical quantization conditions, *Journal of Mathematical Physics* 12: 343-358.

Gutzwiller, M. C. (1977). Bernoulli sequences and trajectories in the anisotropic Kepler problem, *Journal of Mathematical Physics* 18: 806-823.

Gutzwiller, M. C. (1980). Classical quantization of a hamiltonian with ergodic behavior, *Physical Review Letters* 45: 150-153.

Gutzwiller, M. C. (1981). Periodic orbits in the anisotropic Kepler problem, *in* Devaney, R. L. & Nitecki, Z. H. (ed.) *Classical Mechanics and Dynamical systems*, Marcel Dekker, New York, pp. 69-90.

Gutzwiller, M. C. (1982). The quantization of a classically ergodic system, *Physica D* 5: 183-207.

Gutzwiller, M. C. (1990). *Chaos in Classical and Quantum Mechanics*, Springer.

Hannay, J. H. & Ozorio de Almeida, A. M. (1984). Periodic orbits and a correlation function for the semiclassical density of states, *Journal of Physics* A 17: 3429-3440.

Hasegawa, H., Mikeska, H. J. & Frahm, H. (1988). Stochastic formulation of energy-level statistics, *Physical Review* A 38: 395-399.

Heusler, S. et al. (2007). Periodic-orbit theory of level correlations, *Physical Review Letters* 98: 044103,1-4.

Hejhal, D. A. & Rackner, B. N. (1992). On the topography of Maass waveforms for PSL(2,Z), *Experimental Mathematics* 1: 275-305.

Heller, E. J. (1984). Bound-state eigenfunctions of classically chaotic hamiltonian systems: scars of periodic orbits, *Physical Review Letters* 53: 1515-1518.

Heller, E. J. (1989). Wavepacket dynamics and quantum chaology, *in* Giannoni, M. J., Voros A. & Zinn-Justin J. (ed.) *Les Houches Summer School, Session LII, Chaos and quantum physics*, North-Holland, Amsterdam, pp. 547-664.

Huckestein, B. & Schweitzer, L. (1994). Relation between the correlation dimensions of multifractal wave functions and spectral measures in integer quantum Hall systems, *Physical Review Letters* 72: 713-716.

Husimi, K. (1940). Some formal properties of the density matrix, *Proceedings of the Physico-Mathematical Society of Japan* 22: 264-314.

Kravtsov, V. E. et al. (1994). Universal spectral correlations at the mobility edge, *Physical Review Letters* 72: 888-891.

Kravtsov, V. E. & Tsvelik, A. M. (2000). Energy level dynamics in systems with weakly multifractal eigenstates: Equivalence to one-dimensional correlated fermions at low temperatures, *Physical Review* B 62: 9888-9891.

Kustaanheimo, P. & Stiefel, E. (1965). Perturbation theory of Kepler motion based on spinor regularization, *Journal für die reine und angewandte Mathematik* 218: 204-219.

Marcus, C. M. et al. (1992). Conductance fluctuations and chaotic scattering in ballistic microstructures, *Physical Review Letters* 69: 506-509.

Mehta, M. L. (2004). *Random Matrices*, 3rd ed. Academic Press, Amsterdam.

Moshe, M., Neuberger, H. & Shapiro, B. (1994). Generalized ensemble of random matrices, *Physical Review Letters* 73: 1497-1500.

Müller, K. & Wintgen, D. (1994). Scars in wavefunctions of the diamagnetic Kepler problem, *Journal of Physics B: Atomic, Molecular and Optical Physics* 27: 2693-2718.

Pandey, A. (1979). Statistical properties of many particle spectra. Ergodic behaviour in random matrix ensembles, *Annals of Physics* 119: 170-191.

Shklovskii, B. I., Shapiro, B. et al. (1993). Statistics of spectra of disordered system near the metal-insulator transition, *Physical Review* B47: 11487-11490.

Stein, J. & Stöckmann, H. -J. (1992). Experimental determination of billiard wave functions, *Physical Review Letters* 68: 2867-2870.

Sutherland, B. (1971a). Quantum many-body problem in one dimension: Ground state, *Journal of Mathematical Physics* 12: 246-250.

Sutherland, B. (1971b). Quantum many-body problem in one dimension: Thermodynamics, *Journal of Mathematical Physics* 12: 251-256.

Weiss, D. et al. (1991). Electron pinball and commensurate orbits in a periodic array of scatterers, *Physical Review Letters* 66: 2790-2793.

Wigner, E. P. (1951). On the statistical distribution of the widths and spacings of nuclear resonance levels, *Proceedings of the Cambridge Philosophical Society* 47: 790-798.

Wintgen, D., Marxer, H. & Briggs, J. S. (1987). Efficient quantisation scheme for the anisotropic Kepler problem, *Journal of Physics* A 20: L965-L968.

Wintgen, D. & Marxer, H. (1988). Level statistics of a quantized cantori system, *Physical Review Letters* 60: 971-974.

Yukawa, T. & Ishikawa, T. (1989). Statistical theory of level fluctuations, *Progress of Theoretical Physics Supplement* 98: 157-172.

Zaslavsky, G.M. et al. (1991). *Weak Chaos and Quasi Regular Patterns*, Cambridge University Press, Cambridge.

Zirnbauer, M. R. & Haldane, F. D. M. (1995). Single-particle Green's functions of the Calogero-Sutherland model at couplings $\lambda = 1/2$, 1, and 2, *Physical Review* B 52: 8729-8745.

Zirnbauer, M. R. (1996). Supersymmetry for systems with unitary disorder: Circular ensembles, *Journal of Physics* A 29: 7113.

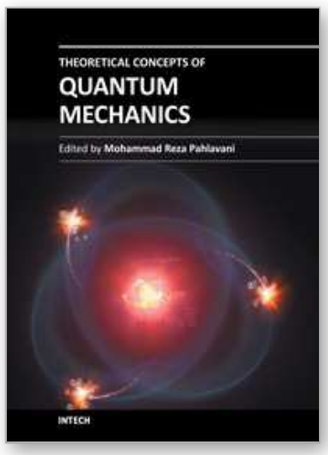

Theoretical Concepts of Quantum Mechanics

Edited by Prof. Mohammad Reza Pahlavani

ISBN 978-953-51-0088-1
Hard cover, 598 pages
Publisher InTech
Published online 24, February, 2012
Published in print edition February, 2012

Quantum theory as a scientific revolution profoundly influenced human thought about the universe and governed forces of nature. Perhaps the historical development of quantum mechanics mimics the history of human scientific struggles from their beginning. This book, which brought together an international community of invited authors, represents a rich account of foundation, scientific history of quantum mechanics, relativistic quantum mechanics and field theory, and different methods to solve the Schrodinger equation. We wish for this collected volume to become an important reference for students and researchers.

How to reference

In order to correctly reference this scholarly work, feel free to copy and paste the following:

Kazuhiro Kubo and Tokuzo Shimada (2012). Anisotropic Kepler Problem and Critical Level Statistics, Theoretical Concepts of Quantum Mechanics, Prof. Mohammad Reza Pahlavani (Ed.), ISBN: 978-953-51-0088-1, InTech, Available from: http://www.intechopen.com/books/theoretical-concepts-of-quantum-mechanics/anisotropic-kepler-problem-and-critical-level-statistics

INTECH
open science | open minds

InTech Europe
University Campus STeP Ri
Slavka Krautzeka 83/A
51000 Rijeka, Croatia
Phone: +385 (51) 770 447
Fax: +385 (51) 686 166
www.intechopen.com

InTech China
Unit 405, Office Block, Hotel Equatorial Shanghai
No.65, Yan An Road (West), Shanghai, 200040, China
中国上海市延安西路65号上海国际贵都大饭店办公楼405单元
Phone: +86-21-62489820
Fax: +86-21-62489821

IntechOpen